Applied Physics Letters

Well-aligned and suspended single-walled carbon nanotube film: Directed self-assembly, patterning, and characterization

Cite as: Appl. Phys. Lett. **94**, 261903 (2009); https://doi.org/10.1063/1.3151850
Submitted: 08 February 2009 . Accepted: 04 May 2009 . Published Online: 29 June 2009

Miao Lu, Min-Woo Jang, Greg Haugstad, Stephen A. Campbell, and Tianhong Cui

Well-aligned and suspended single-walled carbon nanotube film: Directed self-assembly, patterning, and characterization

Miao Lu,[1] Min-Woo Jang,[2] Greg Haugstad,[3] Stephen A. Campbell,[2] and Tianhong Cui[1,a)]
[1]*Department of Mechanical Engineering, University of Minnesota, 1100 Mechanical Engineering 111 Church Street S.E., Minneapolis, Minnesota 55455, USA*
[2]*Department of Electrical and Computer Engineering, University of Minnesota, EECS Building 200 Union Street S.E., Minneapolis, Minnesota 55455, USA*
[3]*Characterization Facility, University of Minnesota, 12 Shepherd Labs, 100 Union St. S.E., Minneapolis, Minnesota 55455, USA*

(Received 8 February 2009; accepted 4 May 2009; published online 29 June 2009)

Self-assembly process, patterning, and characterization of well-aligned single-walled carbon nanotube (SWNT) films are presented in this letter. The dc current in an ac dielectrophoresis of an SWNT solution was measured and used to control the self-assembly process to get an oriented, compact SWNT film 15–20 nm thick. The film was further patterned to form submicron beams by focused ion beams, or lithography and oxygen plasma etching. The Young's modulus of the film ranged from 350 to 830 GPa. The electrical resistivity was about 8.7×10^{-3} Ω cm. The temperature coefficient of resistance was -1.2%/K. © *2009 American Institute of Physics*.
[DOI: 10.1063/1.3151850]

Nanoscale suspended SWNT beam is a fundamental building block for many nanoelectromechanical systems (NEMS) devices such as nano switches, resonators, and biosensors. Compared to Chemical Vapor Deposition (CVD) method,[1] the solution-based approach[2–4] seems to be able to realize lateral alignment without heating the substrate. In the area of SWNTs patterning, some approaches including contact printing,[5] liquid crystalline processing,[6] and lithography plus reactive ion etching[7] were reported. In order to realize a suspended SWNT film, Poly(methyl methacrylate) (PMMA) was used as the sacrificial layer in a previous work.[8] However, the current approaches are not very efficient in forming flat, highly compact, and lateral aligned nanoscale SWNT beams for NEMS applications due to the poor process compatibility, uncontrollable SWNT density, or deformed films. Dielectrophoretic self-assembly of SWNTs is being studied both experimentally[9] and theoretically.[10] Some recent progress focused on the self-assembly of individual SWNTs between two electrodes.[11,12] However, an individual SWNT cannot meet the current capacity or the process controllability requirements of most nanoelectronics or NEMS applications. If the density of oriented SWNTs in a dielectrophoresis process is highly increased, a compact, patternable membrane with a high current capacity can be obtained, while retaining the superior electrical and mechanical properties of SWNTs.

In this letter, a suspended and compact SWNT film was fabricated by a well-controlled dielectrophoresis process without using a sacrificial layer. The film can be patterned to realize suspended nanoscale beams. Finally, the electrical and mechanical characteristics of this suspended SWNT membrane were investigated to provide critical parameters for the design of future NEMS devices.

First, two bilayers of poly(diallyldimethylammonium chloride) (PDDA)/poly(styrenesulfonate) (PSS) and a layer of PDDA were layer-by-layer self-assembled on the silicon dioxide surface between two Cr/Au counter electrodes to make the surface positively charged. Next, 50 μg/ml SWNT (99% purified) water solution from NANOINTEGRIS was put in an ultrasonic bath (80 W, 40 kHz) with the chip immersed in the solution vertically, and an ac electric field (5 MHz, 2 V/μm) was applied. Finally, the chip was rinsed in de-ionized water followed by nitrogen blow drying. A dc voltage of 0.5 V was added on the ac electric field to measure the dc resistance between the two electrodes to timely quantify the number of the assembled SWNTs during the dielectrophoretic self-assembly process. Figures 1(a)–1(c) show the varied dc resistance in the directed self-assembled process with different ac frequencies, ac electric fields, and SWNT solution concentrations. Through the data, a minimized resistance, which means a high dense SWNT film, can be obtained with a concentration of 50 μg/ml, and an electric field of more than 1.5 V/μm at a frequency of higher than 300 kHz. In addtion, the circuit shown in Fig. 1(d) was used to control the density of assembled SWNTs. When the dc current increases to a set point, the analog switch bypasses the ac signal across the electrodes so that the dielectrophoretic assembly is stopped to realize an SWNT film with a desirable density. Figures 1(e) and 1(f) shows the assembled SWNT films with low and high densities connecting two electrodes. In the experiments, the SWNT film across the two electrodes instead of between the electrode and the substrate, and close separate electrodes with sharp projected profiles lead to suspended self-aligned membranes.

As shown in Fig. 2(a), the *G*-band (~1590 cm^{-1}) intensity polarized by the laser parallel to the SWNT alignment direction is ~5.7 times higher than that polarized by the laser perpendicular to SWNT alignment direction, indicating a high degree of alignment. This intensity ratio is higher than the previous result of Raman characterization of a CNT alignment by direct printing (~3.7 times),[13] and lower than that of an aligned SWNT film by Langmuir-Blodgett (LB) assembly (~8times).[14] The *G*-band intensities inclining at 0°, 11.25°, 22.5°, 37.5°, 45°, and 90° to the SWNT align-

a)Electronic mail: tcui@me.umn.edu.

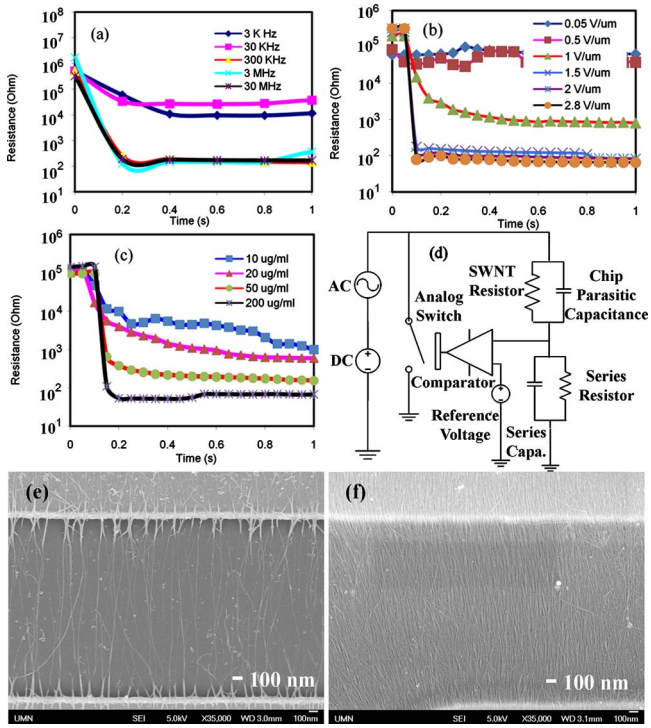

FIG. 1. (Color online) (a) Change of dc resistance between electrodes with different ac frequencies at 100 μg/ml, 2 V/μm; (b) Change of dc resistance between electrodes with different electric fields at 100 μg/ml, 3 MHz; (c) Change of dc resistance between electrodes with different concentrations of SWNT suspensions at 3 MHz, 2 V/μm; (d) Schematic illustration of a controlling circuit, (e), (f) SEM images of SWNT films with different densities through the control of dc currents.

ment direction were shown in Fig. 2(c). Most of SWNTs were found to stay at an angle in a range of 0°–22.5° from the alignment direction. The surface number density of the self-assembled SWNT film is counted in a range of 100 nm using a scanning electron microscopy (SEM) image, resulting in a surface number density of 50–100 bundles/μm, as shown in Fig. 2(d). Compared with the reported surface

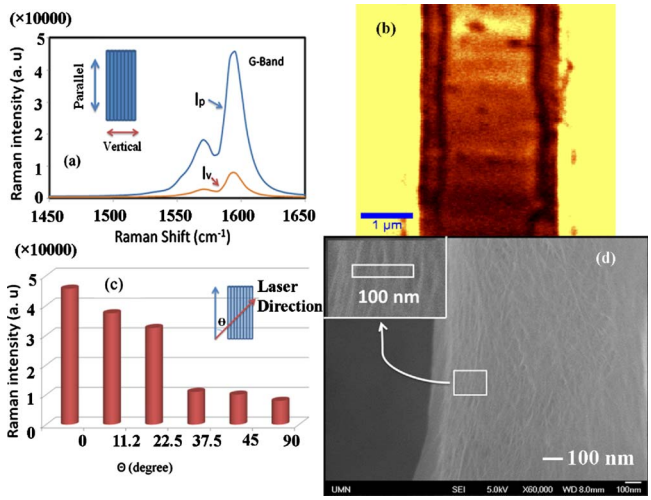

FIG. 2. (Color online) Characterization of alignment and density of an SWNT film by Raman microscope and SEM. (a) *G*-band Raman intensity of parallel to or perpendicular to an SWNT alignment direction. (b) Raman image of the SWNT film. (c) *G*-band Raman intensity with different inclined angels between 0° and 90° with respect to the SWNT alignment direction. (d) SEM images of aligned SWNTs, 5–10 SWNT or SWNT bundles visible in a range of 100 nm.

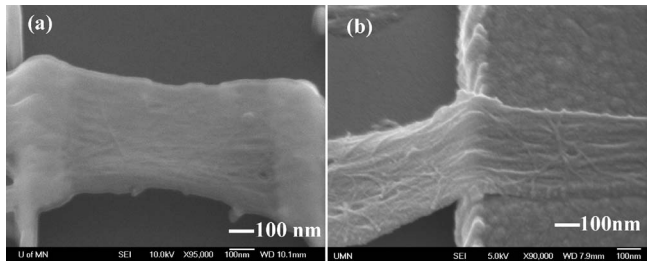

FIG. 3. SEM images of suspended SWNT beams. (Left) Beam patterned by focus ion beam. (Right) Beam patterned by lithography and oxygen plasma etching.

number density of a dense SWNT film by liquid crystalline, in which a surface number density of 18 bundles/μm was demonstrated,[6] the directed self-assembled SWNT film in this paper hs more SWNT bundles, possibly leading to a condense SWNT structure due to the allied electric field. In addition, the dense SWNT film was also verified by a uniform *G*-band Raman imaging, as shown in Fig. 2(b).

Based on densely self-assembled SWNT films, nanoscale suspended SWNT beams were prepared by FIB or photolithography and O_2 plasma etching, as shown in Fig. 3. An FIB (FEI Quanta 200 3D) was used to pattern SWNT membranes at 30 keV and 50 nA. In the oxygen etching process, an STS dry etcher (Model 320) was employed for the patterning at 100 W, 50 mTorr, and 100 sccm oxygen flow for 2 min with a photoresist (Shipley S1813) mask 1.3 μm thick.

As shown in Fig. 4, the mechanical properties of a suspended SWNT beam were measured by atomic force microscopy (AFM) (Digital Instruments Nanoscope III Multimode) using an calibrated AFM cantilever (PointProbe® Plus, Nanosensors, 3.86 N/m). Operating in tapping mode, the sample was approached to the vertically oscillating AFM tip until its amplitude was reduced to zero, and further tested until a particular upward cantilever deflection was achieved. This was performed at two locations, the center of the suspended beam and a rigid sample surface away from the beam. Therefore, two "force curves" were sampled: quasi-static deflection (multiplied by a spring constant) versus *Z* displacement. The spring constant of the SWNT beam,

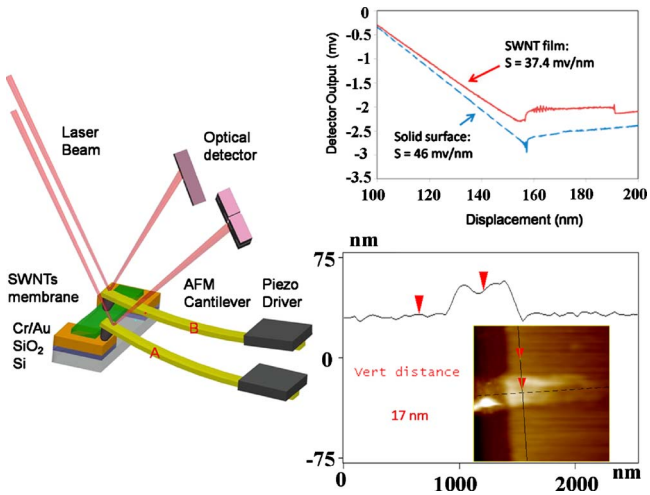

FIG. 4. (Color online) Principle and results of AFM characterization of SWNT beams. (Left) Principle of the spring constant determination. (Upper right) Force curves on a solid surface and on an SWNT beam. (Bottom right) Thickness measurement of an SWNT beam.

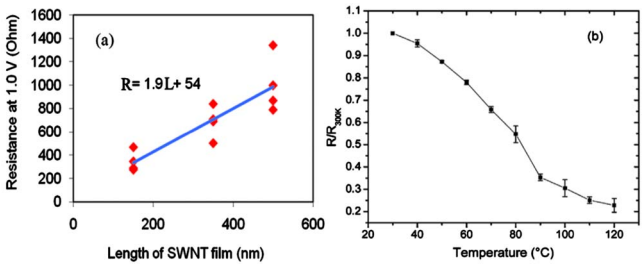

FIG. 5. (Color online) (a) Resistance of SWNT beams with different length, and (b) measurement of TCR of SWNT films from room temperature to 120 °C.

K_{SWNT} was determined by the following equation:

$$K_{SWNT} = \frac{K_{AFMcantilever}}{S_{solidsurface}/S_{SWNT} - 1},$$

where $K_{AFMcantilever}$ is the calibrated spring constant of the AFM cantilever, $S_{solidsurface}$ and S_{SWNT} are the slope of the force curve on the solid surface and at the center of SWNT cantilever, respectively.[15] The spring constant of the SWNT beam was determined to be 16.8 N/m by multiple tests. The dimensions of the beam measured by SEM are 950 nm long and 320 nm wide. The thickness was measured to be in a range from 15 to 20 nm by AFM. The expression for calculating the Young's modulus of a two-end fixed beam with a central point load is given by

$$E = \frac{kL^3}{16wt^3},$$

where E is the Young's modulus, k is the spring constant, and L, w, and t are the length, width, and thickness of the beam, respectively. Using the above data in this expression, we compute the Young's modulus of the SWNT membrane to be from 350 to 830 GPa due to the thickness variation. This result is higher than the report Young's modulus (100 GPa) of SWNT ropes.[16] and is far larger than the reported Young's modulus (35 GPa) of SWNT layer-by-Layer film by *et al.*[17] The electric field induced SWNT condensation is one possible reason resulting in a higher Young's modulus. For example, Mureau *et al.* demonstrated SWNTs concentrated and trapped by an electric field through fluorescence imaging.[18]

The *I-V* properties of three types of SWNT beams with the same contact area and different dimensions were tested [Fig. 5(a)]. The width of the SWNT beams is 3 μm and the length of the beams are 150, 350, and 500 nm respectively, and the average thickness is measured by AFM as ~17 nm. At a bias of 1.0 V, the resistance R of the film is found to fit the equation: $R=1.9\ \Omega/\text{nm}\times L+54\ \Omega$, where L is the length of the beam with the unit of nanometer. From the slope of the equation and the dimensions of the film, the resistivity of the SWNT film is about $8.7\times10^{-3}\ \Omega$ cm. Thess *et al.* calculated the resistivity of ropes of metallic SWNTs to be in an order of $10^{-4}\ \Omega$ cm at 300 K,[19] and the resistivity of SWNTs in the alignment direction by a direct printing is $2.32\times10^{-3}\ \Omega$ m.[13] Li *et al.*[14] reported an aligned Hipco SWNT film with a resistance of more than 25 times higher than the aligned laser-ablation SWNT film by the LB assembly. This resistivity difference is possibly due to different SWNTs used in these experiments and different alignment approaches leading to a variation in SWNTs interactions. The TCR was measured to be −1.2%/K from room temperature to 120 °C [Fig. 5(b)]. The value is higher than that in previous report (−0.7%/K at 300 K),[20] which proved that the aligned SWNT film is a promising material for possible thermal or infrared applications.

In conclusion, well-aligned and suspended SWNT films were deposited by a controllable dielectrophoretic self assembly. The dense films were patterned to form nanoscale beams by FIB or lithography and oxygen plasma etching. The mechanical properties were characterized by AFM, and the electrical performance of the membranes was also tested. This new process for creating a suspended SWNT beam can be integrated into the fabrication of NEMS devices, and is believed to be very promising for a variety of potential applications including nanoswitches, nanoresonators, and biosensors.

This work was partially supported by the DARPA NEMS Program. We also acknowledge the Nanofabrication Center and the Characterization at the University of Minnesota Facility, which are supported by NSF through NNIN. In particular, we thank Dr. Jinping Dong for the valuable discussion and help on the characterization of SWNT alignment using Raman microscope. DARPA through SPAWAR Grant No. N66001–07–1–2060; NSF NNIN is Grant No. ECS-0335765.

[1] M. Terrones, N. Grobert, J. Olivares, J. P. Zhang, H. Terrones, K. Kordatos, W. K. Hsu, J. P. Hare, P. D. Townsend, K. Prassides, A. K. Cheetham, H. W. Kroto, and D. R. M. Walton, Nature (London) **388**, 52 (1997).
[2] A. H. Monica, S. J. Papadakis, R. Osiander, and M. Paranjape, Nanotechnology **19**, 085303 (2008).
[3] M. C. LeMieux, M. Roberts, S. Barman, Y. W. Jin, J. M. Kim, and Z. Bao, Science **321**, 101 (2008).
[4] R. Krupke, F. Hennrich, M. M. Kappes, and H. V. Lohneysen, Nano Lett. **4**, 1395 (2004).
[5] M A. Meitl, Y. Zhou, A. Gaur, S. Jeon, M. L. Usrey, M. S. Strano, and J. A. Rogers, Nano Lett., **4**, 1643 (2004).
[6] H. Ko and V. V. Tsukruk, Nano Lett. **6**, 1443 (2006).
[7] Y. Hayamizu, T. Yamada, K. Mizuno, T. Davis, D. N. Futaba, M. Yumura, and K. Hata, Nat. Nanotechnol. **3**, 289 (2008).
[8] S. W. Lee, D. S. Lee, H. Y. Yu, E. E. B. Campbell, and Y. W. Park, Appl. Phys. A: Mater. Sci. Process. **78**, 283 (2004).
[9] X. Q. Chen, T. Saito, H. Yamada, K. Matsushige, Appl. Phys. Lett., **78**, 3714 (2001).
[10] M. Dimaki and P. Bøggild, Nanotechnology **15**, 1095 (2004).
[11] S. Banerjee, B. E. White, L. Huang, B. J. Rego, S. O'Brien, and I. P. Herman, J. Vac. Sci. Technol. B **24**, 3173 (2006).
[12] L. F. Dong, V. Chirayos, J. Bush, J. Jiao, V. M. Dubin, M. V. Chebian, Y. Ono, J. F. Conley, Jr., and B. Ulrich, J. Phys. Chem. B **109**, 13148 (2005).
[13] J. Im, Il-Ha. Lee, B. Y. Lee, B. Kim, J. Park, W. Yu, U. J. Kim, Y.H. Lee, M-J. Seong, E. H. Lee, Y-S. Min, and S. Hong, Appl. Phys. Lett. **94**, 053109 (2009).
[14] X. L. Li, L. Zhang, X. R. Wang, I. Shimoyama, X. M. Sun, W. S. Seo, and H. J. Dai, J. Am. Chem. Soc. **129**, 4890 (2007).
[15] P. J. Cumpson, J. Hedley, and P. Zhdan, Nanotechnology **14**, 918 (2003).
[16] J. P. Salvetat, G. A. D. Briggs, J. M. Bonard, R. R. Basca, A. J. Kulik, T. Stöckli, N. A. Burnham, and L. Forró, Phys. Rev. Lett. **82**, 944 (1999).
[17] A. A. Mamedov, N. A. Kotov, M. Prato, D. M. Guldi, J. P. Wicksted, and A. Hirsck, Nature Mater. **1**, 190 (2002).
[18] N. Mureau, E. Mendoza, and S. R. P. Silva, Electrophoresis **28**, 1495 (2007).
[19] A. Thess, R. Lee, P. Nikolaev, H. J. Dai, P. Petit, J. Robert, C. H. Xu, Y. H. Lee, S. G. Kim, A. G. Rinzler, D. T. Colbert, G. Scuseria, D. Tománek, J. E. Fischer, and R. E. Smalley, Science **273**, 483 (1996).
[20] J. H. Chen, E. Costan, M. A. van Huis, Q. Xu, and H. W. Zandbergen, Science **312**, 416 (2006).